Phase-difference-based 3-D Source Localization Using a Compact Receiver Configuration

Hui Chen, Tarig Ballal and Tareq Y. Al-Naffouri
Computer, Electrical and Mathematical Science & Engineering
King Abdullah University of Science and Technology (KAUST), Thuwal, 23955-6900
Email: {hui.chen; tarig.ahmed; tareq.alnaffouri}@kaust.edu.sa

***Abstract*—Source localization has many important applications, especially in tracking and navigation. Trilateration, triangulation, and multilateration are three widely-used techniques for localization depending on the available information. The main drawbacks of these methods are the requirements of a large number of anchors and an elaborately designed layout. To accomplish the localization task with minimal resources while maintaining reasonable accuracy, we propose a 3-D source localization method with a compact infrastructure (prototype realized with 4 anchors located within an area of 2.5×20 cm^2) by utilizing only phase-difference information. The proposed method first estimates the direction-of-arrival (DOA) of the target and then finds the candidate 3-D location along on the DOA by minimizing a cost function. This system is compared to the other two similar setups based on simulations and the experimental tests are carried out using acoustic waves. The results show that the proposed approach can achieve 3-D location error of 2.77 cm for a target at 0.5 m without synchronization between the transmitter and the receivers. The relatively small system size and sufficient location accuracy provide possibilities in controller tracking for virtual reality applications.**

I. Introduction

Location information is important for many applications such as patient tracking [1], robot navigation [2], wireless sensor network (WSN) [3], gesture recognition [4] and so on. Sensor network based localization is one of the important methods to obtain the location of a target using a base station (BS) network; a summary of techniques can be found in [5]. Trilateration can be implemented using measurements of the distance from the target to the BS. The distance can be estimated using received signal strength (RSS) [6], time of flight (TOF) [7], or round-trip TOF [8]. Triangulation algorithms are used in systems that can utilize the direction of arrival (DOA) information of the signal to the BSs [9]. When the BSs are synchronized, multilateration algorithms can be applied using time difference of arrival (TDOA) information [10].

Although deploying sensor networks yield sufficient localization accuracy, the number of BSs required in these methods increases the complexity and the cost of the system. As an alternative, a localization solution using a single base station is of great utility. Several positioning systems using single BS were designed in [11]–[13]. These systems are still unsatisfactory either because of their poor accuracy or the large system size.

To solve the mentioned high complexity and large size issues while accomplishing the localization task with satisfactory measurement accuracy, we proposed a system using phase-difference measurement and a compact receiver configuration. The definition of **compact** has two aspects:

a) Minimum hardware resources, i.e., the system functions with at most 4 anchors without synchronization between the transmitter and the receivers;

b) Minimum efforts for deployment. The small size of the receiver array (2.5×20 cm^2 for the proposed system) enables the integration of all the components in one board.

This plug-and-use feature prevents calibration errors in system deployment. And the small size of the array can be easily installed on a virtual reality headset to track the 3D locations of the controllers.

Due to the small distance between the anchors, TDOA information is no more helpful in finding 3-D location. This system estimates the DOA and absolute range of a target by using only the phase-difference information which will be explained in the next section. The proposed methods can be applied to both acoustic and radio frequency signals with possible application in indoor localization, human-computer interaction, robot navigation, and so on.

This paper is organized as follows. Section II states the localization model and explains the 3-D localization algorithm. Section III analyzes how locating performance is affected by the system parameters and gives suggestions on tracking application. Section IV presents simulation and experimental results. In section V, we derive the conclusions of the whole work with suggestions of future directions.

II. The Proposed Localization Algorithm

A. Localization and Signal Models

The localization model is shown in Fig. 1. A transmitter periodically sends signal blocks which are received by a planar receiver array on a base station. Each block consists of sinusoidal pulses with frequencies of $f_1, f_2, ..., f_N$, where N is the number of frequency components. These pulses have the same duration t_p and are transmitted sequentially inside each block. The transmitted signal block can be expressed in the continuous time (t) domain as

$$x(t) = \sum_{i=1}^{N} a_i(t) \cos(2\pi f_i t + \rho_i), \tag{1}$$

where $a_i(t) = A_i$ for $t \in \{(i-1)t_p, it_p\}$ and zero otherwise; A_i and ρ_i are the amplitude and phase parameters of pulse i.

The receiver array contains a 2-D circular DOA subarray (the locations are denoted as U_1, U_2, U_3) centered at O for DOA estimation and one ranging receiver located at V with a relatively larger distance from O. Thus, forming a far-field model (for DOA estimation) and a near-field model (for range estimation) [12], [14]. This is the minimum number of receivers required to fulfill 3-D localization. However, the number of anchors can be increased to improve performance.

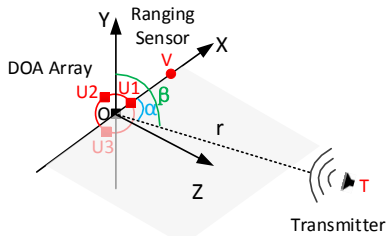

Fig. 1. Localization model.

1) DOA Model: A summary of DOA algorithms can be found in [15], and with a minimum number of three anchors in a DOA array, the unit 3-D direction vector of the target T can be expressed as

$$\mathbf{t} = [\cos(\alpha), \cos(\beta), \cos(\gamma)], \tag{2}$$

where $\cos(\gamma)$ is dependent on α and β which equals to $\sqrt{1-\cos^2(\alpha)-\cos^2(\beta)}$. In the rest of this paper we will focus on the ranging part with known DOA information.

2) Range Model: The ranging anchor V is used to estimate the range r between the target T and the DOA array center O and hence the 3-D location $\mathbf{T}$ can be obtained as

$$\mathbf{T} = r\mathbf{t}. \tag{3}$$

3) Path Difference Model: We define plane w as the plane containing the X-axis (OU_1V) and the direction vector (OT) from DOA array to the transmitter. Then, the 3-D localization problem can be transformed into a ranging problem to estimate the distance r in a 2-D plane w, as shown in Fig. 2; where O is the center of the DOA array, U_1 and V are the anchors laying on the plane w. With known DOA α, $u = OU_1$, and $v = OV$, the distance between the transmitter and the DOA array $r = OT$ can be obtained from the mentioned parameters.

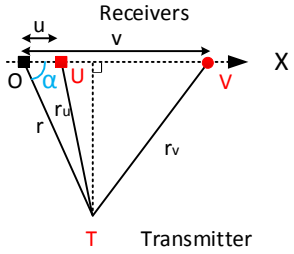

Fig. 2. Ranging model on plane w.

For a target T at a range r, the distance between the target location T and anchor U and V can be expressed as

$$r_u(\alpha, r) = \sqrt{(u - r\cos(\alpha))^2 + (r\sin(\alpha))^2}, \tag{4}$$

$$r_v(\alpha, r) = \sqrt{(v - r\cos(\alpha))^2 + (r\sin(\alpha))^2}. \tag{5}$$

The relationship between the unwrapped phase difference $\phi_n(\alpha, r)$ of frequency f_n and the path difference $p = r_u - r_v$, of the signals received at anchor U and V can be expressed as

$$\begin{aligned} p(\alpha, r) = \frac{\phi_n(\alpha, r)c}{2\pi f_n} &= r_u(\alpha, r) - r_v(\alpha, r) \\ &= \sqrt{u^2 + r^2 - 2ur\cos(\alpha)} - \sqrt{v^2 + r^2 - 2vr\cos(\alpha)}, \end{aligned} \tag{6}$$

where c is the propogation speed of the signal. The derivative of $p(\alpha, r)$ with respect to r can be expressed as

$$\begin{aligned} \frac{\partial p}{\partial r} &= \frac{r - u\cos(\alpha)}{\sqrt{u^2 + r^2 - 2ur\cos(\alpha)}} - \frac{r - v\cos(\alpha)}{\sqrt{v^2 + r^2 - 2vr\cos(\alpha)}} \\ &= \frac{(r - u\cos(\alpha))\sqrt{(r - v\cos(\alpha))^2 + (v\sin(\alpha))^2}}{\sqrt{u^2 + r^2 - 2ur\cos(\alpha)}\sqrt{v^2 + r^2 - 2vr\cos(\alpha)}} \\ &\quad - \frac{(r - v\cos(\alpha))\sqrt{(r - u\cos(\alpha))^2 + (u\sin(\alpha))^2}}{\sqrt{u^2 + r^2 - 2ur\cos(\alpha)}\sqrt{v^2 + r^2 - 2vr\cos(\alpha)}}. \end{aligned} \tag{7}$$

For all $\alpha \in (0, \pi)$ and $r > v > u > 0$, the following pair of inequalities hold

$$(r - u\cos(\alpha))v\sin(\alpha) > (r - v\cos(\alpha))u\sin(\alpha) > 0, \tag{8}$$

and hence the result of equation (7) is positive. This means that for a fixed α, if the value of the estimated unwrapped phase difference $\hat{\boldsymbol{\phi}}$ is known, there exists only one value $\hat{r}$ corresponding to $p(\alpha, r)$ and $\phi_n(\alpha, r)$. The range can be estimated as

$$\hat{r} = \underset{r_m}{\operatorname{argmin}} \sum_{n=1}^{N} |\hat{\phi}_n - \phi_n(\alpha, r_m)|. \tag{9}$$

B. Localization Algorithm

1) Phase-difference Estimation: The path difference (unwrapped phase difference), however, can not be obtained in most of the cases. The observed phase-difference vector $\hat{\boldsymbol{\psi}}$ from the two anchors is wrapped into $[-\pi, \pi)$ [16], [17] as

$$\begin{aligned} \hat{\psi}_n = \text{wrap}(\hat{\phi}_n) &= \text{mod}(\hat{\phi}_n + \pi, 2\pi) - \pi \\ &= \text{ang}(Y_u(f_n) \cdot Y_v^*(f_n)), \end{aligned} \tag{10}$$

where $\hat{\psi}_n$ is the observed phase-difference at frequency f_n, Y_u and Y_v are the Discrete Fourier Transform (DFT) of the received signals at anchor U and anchor V respectively, $\hat{\phi}$ is the noisy unwrapped phase-difference, $\text{mod}(a, b)$ returns the remainder after division of a by b.

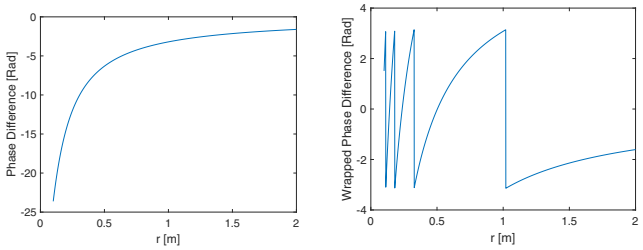

(a) $\phi(r)$ (b) $\psi(r)$

Fig. 3. An example of a) unwrapped; and b) the corresponding wrapped phase difference.

2) Range Estimation: One example of the phase-wrapping problem of a single frequency signal is shown in Fig. 3 where (a) is the unwrapped phase-difference $\phi(\alpha, r)$ and (b) is the wrapped phase-difference $\psi(\alpha, r)$. If the signal has multiple frequencies $\mathbf{f} = [f_1, ..., f_N]^T$, the observed phase-difference can be differentiated from different ranges. As a consequence, a grid search method can be used to find the estimated range $\hat{r}$. Namely, we search the range in a candidate set $[r_1, r_2, ..., r_M]$ along the DoA of α and find the range that matches the observations best. In this way, the estimation in 3-D space is simplified into a 1-D problem which reduces the algorithm complexity. This candidate set can be chosen, for example, with an increment of 1 cm from 0.3 m to 4 m, depends on the requirement of detecting range and compulational resources. For a hypothesized range r_m, the corresponding observed phase-difference vector $\boldsymbol{\psi} = [\psi_1, ..., \psi_N]^T$ can be calculated based on (6) as

$$\psi_n(\alpha, r_m) = \text{wrap}(\phi_n(\alpha, r_m)) = \text{wrap}\left(\frac{p(\alpha, r_m) 2\pi f_n}{c}\right), \tag{11}$$

and the estimated range $\hat{r}$ can be obtained by finding the candidate that minimizes the cost function $e(\alpha, r_m)$ as

$$\begin{aligned} \hat{r} &= \underset{r_m}{\text{argmin}}\ e(\alpha, r_m) \\ &= \underset{r_m}{\text{argmin}} \sum_{n=1}^{N} |\text{wrap}(\hat{\psi}_n - \psi_n(\alpha, r_m)|. \end{aligned} \tag{12}$$

This equation is the same as (9) if no phase-wrapping happens. It also applies to a receiver array with more than one ranging anchor by introducing more wrapped phase-difference vectors into the cost function.

3) Sufficient condition: In noise free case, a **sufficient condition** that equation (12) holds is that two target locations r and $r + \Delta r$ do not have the same wrapped phase difference. Or otherwise they will not be differentiable, which can be expressed as

$$\begin{aligned} \text{wrap}(\boldsymbol{\phi}(\alpha, r)) &\neq \text{wrap}(\boldsymbol{\phi}(\alpha, r + \Delta r)) \\ &\neq \text{wrap}(\boldsymbol{\phi}(\alpha, r) + \Delta\boldsymbol{\phi}). \end{aligned} \tag{13}$$

where $\Delta\boldsymbol{\phi} = [\Delta\phi_1, ..., \Delta\phi_N]^T = \boldsymbol{\phi}(\alpha, r + \Delta r) - \boldsymbol{\phi}(\alpha, r)$. Since $p(\alpha, r)$ is linearly increasing with r and based on equation (6) we can have

$$0 < \Delta\phi_n = \Delta p \frac{2\pi f_n}{c} < \frac{\Delta p_{max}}{c} 2\pi f_n, \tag{14}$$

where $\Delta p = p(\alpha, r + \Delta r) - p(\alpha, r)$, $\Delta p_{max} = p(\alpha, r_{max}) - p(\alpha, r_{min})$, r_{max} and r_{min} are the maximum and minimum locating distance that can be predefined. Based on equation (13) and (14), the sufficient condition can be expressed as that equation (15) is not satisfied for all the possible value of g_n.

$$\Delta\phi_n = \Delta p \frac{2\pi f_n}{c} = 2\pi g_n, \tag{15}$$

where $g_n \in 1, 2, ..., \text{ceil}(2\pi f \Delta p_{max}/c)$ is a positive integer.

A simplified version of a **sufficient condition** is that **equation** (16) **is not satisfied**.

$$\frac{f_1}{g_1} = \frac{f_2}{g_2} = ... = \frac{f_N}{g_N}. \tag{16}$$

C. 3-D Localization Algorithm Summary

This method estimates 3-D location based on a direction unit vector and a distance. The 3-D localization algorithm can be summarized as following:

1. Obtain direction vector $\mathbf{t}$ and α using DOA algorithm;
2. Calculate the wrapped phase-difference vector $\hat{\boldsymbol{\psi}}$ using (10);
3. Define range candidates set $[r_1, r_2, ..., r_M]$ and calculate the corresponding observed phase-difference $\boldsymbol{\psi}(r_m)$ of all the range candidates using (11);
4. Calculate the estimated range $\hat{r}$ using (12);
5. Obtain the 3-D location of the target as $\hat{r} \cdot \mathbf{t}$ using (3).

III. Error Model and Tracking Strategy

A. System Parameters Analysis

The system performance is affected by a various of factors such as target range r, snr, target direction α, anchor distance u, v, signal frequency $\mathbf{f}$ and so on. To have a better understanding of these factors, we will visualize the wrapped phase-difference vector of the candidate set $\boldsymbol{\psi}(\alpha, r_m)$. For simplicity, N is chosen as 2 and the visualization is shown in Fig.4 (a) with some highlighted candidates. The parameters are set as $\alpha = 90^o$, $u = 0.9$ cm, $v = 14$ cm, $\mathbf{f} = [18, 21]^T$ kHz and r_m is chosen from 0.2 m to 3 m with an increment of 0.01 m.

1) snr, r: The basic idea of range estimation in (12) is that, given an estimated $\hat{\boldsymbol{\psi}}$, we are looking for a point $\boldsymbol{\psi}(\alpha, \hat{r})$ in a points set $\boldsymbol{\psi}(\alpha, r_m)$ which has the least Manhattan distance to $\hat{\boldsymbol{\psi}}$. Take a target at 0.26 m for example, if a noisy phase-difference is inside the red area, the estimation range will have the error smaller than $0.01m$. As the points are getting closer when r increases, performance deteriorate because the red area is smaller (indicates a smaller probability to have a small error). This is also easy to understand intuitively because the setup tends to be a far-field model when r is large.

2) v: The visualization of $v = 0.2$ m is shown in Fig.4 (b). A larger v will sparse the candidates. It indicates a better result based on our previous conclusion. However, the inconvenience of deployment is beyond our 'minimum infrastructure' purpose. Also, the directionality of the transducer and the signal attenuation for large v also decrease the performance.

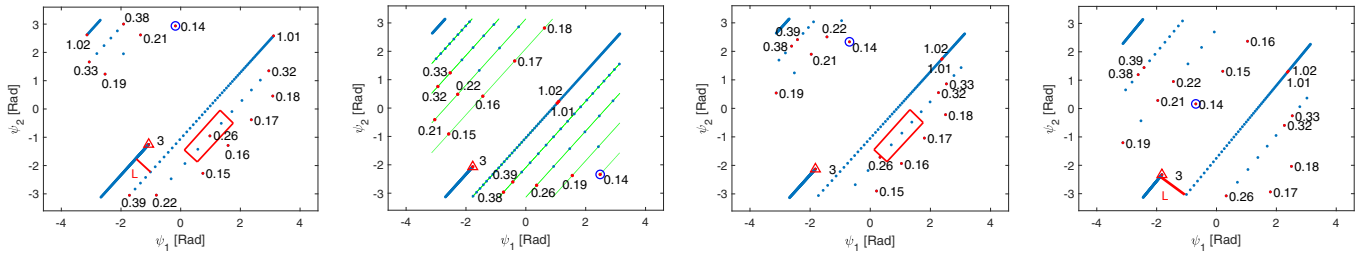

Fig. 4. The visualization of $\psi(\alpha, r_m)$. (a) Original $\psi(\alpha, r_m)$ with $\alpha = 90^{\text{o}}$, $u = 0.9$ cm, $v = 14$ cm, $\mathbf{f} = [18, 21]^T$ kHz; (b) $v = 20$ cm; (c) $\alpha = 91^{\text{o}}$; (d) $\mathbf{f} = [18, 23]^T$ kHz.

3) α, u: Another set of $\psi(\alpha, r_m)$ is shown in Fig.4 (c) with the only change on $\alpha = 91^{\text{o}}$. The locations are shifted compared with Fig.4 (a) and hence error occurs. DOA estimation error will not be discussed in this work.

4) $\mathbf{f}$: For $\mathbf{f} = [18, 23]^T$ kHz, $\psi(\alpha, r_m)$ is shown in Fig. 4 (d). A larger distance L between two lines is showing a better performance. However, with the increase of the bandwidth of the frequency $(f_N - f_1)$, the result can be worsened because the large candidate points and small candidate points will interfere with each other. This can be solved by introducing more frequency components or changing the candidate range set, for example, to $(0.3, 3)$ m.

B. Error Level Model

It is difficult to develop an error model containing all the system parameters. Therefore, we will create a simple error level model to evaluate system performance. Given u, v and $\lambda = c/f_c$ where f_c is the signal central frequency, the error level $g(\alpha, r)$ can be defined as

$$g(\alpha, r) = \frac{\lambda}{p'(\alpha, r)}. \tag{17}$$

The value $g(\alpha, r)$ indicates the range estimation error caused by unit wavelength error in phase-difference estimation at r. One example of the error level is shown in Fig. 5 which reflects the system performance at different locations. From the figure, we can see that the error increases when the range r is large and DOA α is far from 90^o.

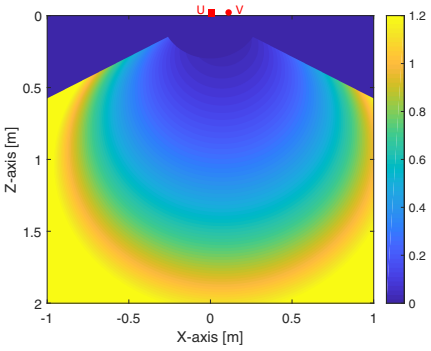

Fig. 5. Error level at different locations on plane w. ($u = 0.9$ cm, $v = 20$ cm, $f_c = 18$ kHz).

C. 3-D Tracking Strategy

We can find that the locating performance drops sharply with the target distance r. In addition, the Doppler effect of the moving target will also degenerate the range estimation. The strategy of implementing this system in 3-D tracking system is 'tracking after synchronizing' by taking the first several measurements as initial range estimation $\hat{r}_0$, and using the relative movements obtained by cross correlation to obtain the rest of the range estimation as

$$\hat{r}_i = \hat{r}_0 + \Delta\hat{r}_i = r_i + \delta r, \tag{18}$$

where $\Delta\hat{r}_i$ is the relative movement of the i-th sample calculated by cross-correlation [7]. The drawback of this solution, however, is that the initial estimation error δr will be added in the following location estimations as $(r + \delta r)\mathbf{t}$.

IV. Simulation and Experiments

A. Simulation Results

We compared the proposed 4-anchor setup (see Fig. 1) with DOA method in [9] which uses 6 anchors as shown in Fig. 6 (a). We match this setup by extending our method to the 6-anchor setup shown in Fig. 6 (b). DOA estimation is based on the method in [18] with a search resolution of 0.5^{o}. The signal frequencies are chosen as $f = [18, 19.5, 21]^T$ kHz for $N = 3$, $f = [18, 21]^T$ kHz for $N = 2$. Other parameters are chosen as $u = 0.9$ cm, $v = 20$ cm, $\alpha = 90^{\text{o}}$ and $SNR = 10$ dB for all the three methods. The simulation results are shown in Fig. 7, which show that the proposed 4-anchor solution is having a satisfactory performance compared to the method from [9]. Performance can be improved by using more anchors and more signal frequencies.

(a) 6-anchor setup from [9] (b) Proposed 6-anchor setup.

Fig. 6. 6-anchor setups used in simulations.

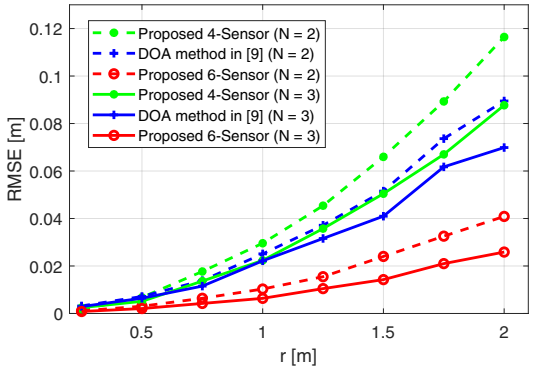

Fig. 7. RMSE for different methods and frequencies.

B. Fixed Points Experimental Results

The experimental tests were carried out in a typical room environment with an indoor temperature of 24^oC. The transmitted ultrasonic signal contains three pulses with each pulse lasts 2 ms and has an update rate of 50 Hz. The sampling frequency is 96 kH and the transmitted signal is chosen the same as simulation parameters with $N = 3$. The transmitter, as well as the BSs were placed 1 m above the ground.

The experimental tests have two parts. In the fixed-DOA test, seven points are chosen in the direction vector $[0, 0, 1]$ with ranges from 0.5 m to 1.5 m. In fixed-range test, points are chosen with direction vector as $[\cos(\alpha), 0, \sin(\alpha)]$. The SNR is around 20 dB at 1 m distance and 500 independent measurements were obtained at each point. The results of fixed-DOA and fixed-range tests are shown in Fig. I where we can find the performance drops fast with r and DOA. However, the accuracy can be improved with more anchors, frequencies, larger v or averaging multiple estimations. Consider the application of tracking virtual reality controllers where the distance between user's hands and head is usually within 1 meter, this system provides sufficient tracking accuracy without introducing extra hardware resources for synchronization between the transmitter and the receivers.

TABLE I
EXPERIMENTAL TEST RESULTS

Range [m]	RMSE [cm]	DOA [^{o}]	RMSE [cm]
0.50	2.77	80	7.13
0.75	3.55	90	5.83
1.00	5.83	100	10.12
1.25	10.65	110	11.64
1.50	15.08	120	22.23

V. CONCLUSION

In this paper, a 3-D positioning system is proposed by utilizing a compact receiver setup. This system can accomplish the localization task with a compact 4-anchor receiver array without synchronization between the transmitter and the receivers. This reduces the hardware and computational complexity, as well as the installation cost of the system.

Several factors affecting the system performance are discussed and a 'tracking after synchronization' strategy is suggested. Simulation and experimental tests demonstrate good performance of the proposed system.

REFERENCES

[1] L. Wan, G. Han, L. Shu, S. Chan, and T. Zhu, "The application of doa estimation approach in patient tracking systems with high patient density," *IEEE Transactions on Industrial Informatics*, vol. 12, no. 6, pp. 2353–2364, 2016.

[2] Y. Li and E. B. Olson, "Extracting general-purpose features from lidar data," in *Robotics and Automation (ICRA), 2010 IEEE International Conference on*. IEEE, 2010, pp. 1388–1393.

[3] P. Nayak and A. Devulapalli, "A fuzzy logic-based clustering algorithm for wsn to extend the network lifetime," *IEEE sensors journal*, vol. 16, no. 1, pp. 137–144, 2016.

[4] H. Chen, T. Ballal, A. H. Muqaibel, X. Zhang, and T. Y. Al-Naffouri, "Air-writing via receiver array based ultrasonic source localization," *IEEE Transactions on Instrumentation and Measurement*, 2020.

[5] A. Lindo, E. Garcia, J. Ureña, M. del Carmen Perez, and A. Hernandez, "Multiband waveform design for an ultrasonic indoor positioning system," *IEEE Sensors Journal*, vol. 15, no. 12, pp. 7190–7199, 2015.

[6] M. Passafiume, S. Maddio, M. Lucarelli, and A. Cidronali, "An enhanced triangulation algorithm for a distributed rssi-doa positioning system," in *Radar Conference (EuRAD), 2016 European*. IEEE, 2016, pp. 185–188.

[7] M. M. Saad, C. J. Bleakley, and S. Dobson, "Robust high-accuracy ultrasonic range measurement system," *IEEE Transactions on Instrumentation and Measurement*, vol. 60, no. 10, pp. 3334–3341, 2011.

[8] B. Liu, H. Chen, Z. Zhong, and H. V. Poor, "Asymmetrical round trip based synchronization-free localization in large-scale underwater sensor networks," *IEEE Transactions on Wireless Communications*, vol. 9, no. 11, pp. 3532–3542, 2010.

[9] M. S. Brandstein, J. E. Adcoßck, and H. F. Silverman, "A closed-form location estimator for use with room environment microphone arrays," *IEEE transactions on Speech and Audio Processing*, vol. 5, no. 1, pp. 45–50, 1997.

[10] H. Chen, T. Ballal, N. Saeed, M.-S. Alouini, and T. Y. Al-Naffouri, "A joint tdoa-pdoa localization approach using particle swarm optimization," *IEEE Wireless Communications Letters*, 2020.

[11] E. O. Dijk, C. Van Berkel, R. M. Aarts, and E. J. van Loenen, "3-d indoor positioning method using a single compact base station," in *Pervasive Computing and Communications, 2004. PerCom 2004. Proceedings of the Second IEEE Annual Conference on*. IEEE, 2004, pp. 101–110.

[12] A. Pourmohammad and S. M. Ahadi, "Real time high accuracy 3-d PHAT-based sound source localization using a simple 4-microphone arrangement," *IEEE Systems Journal*, vol. 6, no. 3, pp. 455–468, 2012.

[13] W. Mao, J. He, and L. Qiu, "Cat: high-precision acoustic motion tracking," in *Proceedings of the 22nd Annual International Conference on Mobile Computing and Networking*. ACM, 2016, pp. 69–81.

[14] J. R. Gonzalez and C. J. Bleakley, "High-precision robust broadband ultrasonic location and orientation estimation," *IEEE Journal of selected topics in Signal Processing*, vol. 3, no. 5, pp. 832–844, 2009.

[15] H. Krim and M. Viberg, "Two decades of array signal processing research: the parametric approach," *IEEE signal processing magazine*, vol. 13, no. 4, pp. 67–94, 1996.

[16] T. Ballal and C. J. Bleakley, "Phase-difference ambiguity resolution for a single-frequency signal," *IEEE Signal Processing Letters*, vol. 15, pp. 853–856, 2008.

[17] ——, "Phase-difference ambiguity resolution for a single-frequency signal in the near-field using a receiver triplet," *IEEE Transactions on Signal Processing*, vol. 58, no. 11, pp. 5920–5926, 2010.

[18] H. Chen, T. Ballal, M. Saad, and T. Y. Al-Naffouri, "Angle-of-arrival-based gesture recognition using ultrasonic multi-frequency signals," in *Signal Processing Conference (EUSIPCO), 2017 25th European*. IEEE, 2017, pp. 16–20.